D'Elia, Valentina et al., 2018. Gold nanorods as SERS substrate for the ultratrace detection of cocaine in non-pretreated oral fluid samples. Colloids and surfaces. A, Physicochemical and engineering aspects, 557, pp.43–50.

Available at https://doi.org/10.1016/j.colsurfa.2018.05.068

Gold nanorods as SERS substrate for the ultratrace detection of cocaine in non-pretreated oral fluid samples

Valentina D'Elia[a], Jorge Rubio Retama[b], Fernando E. Ortega-Ojeda[a], Carmen García Ruiz[a], Gemma Montalvo[a,*]

[a] *Department of Analytical Chemistry, Physical Chemistry and Chemical Engineering University of Alcalá, Ctra. Madrid-Barcelona Km. 33.6, 28871, Alcalá de Henares (Madrid) Spain, and*
University Institute of Research in Police Sciences (IUICP), University of Alcalá, Ctra. Madrid-Barcelona Km. 33.6, 28871, Alcalá de Henares (Madrid) Spain.
[b]*Department of Chemistry in Pharmaceutical Sciences, Faculty of Pharmacy, Complutense University of Madrid, Plaza Ramón y Cajal, 28040 Madrid, Spain*

[*] *Corresponding author - Email: gemma.montalvo@uah.es; Work Phone +34918854671*
Website: www.inquifor.uah.es

ABSTRACT

This work shows the capability of surface-enhanced Raman spectroscopy (SERS) to detect ultratraces of cocaine (COC) in oral fluid (OF). It proposes a new solid substrate made of gold nanorods (Au NRs) to perform sensitive analyses of this complex matrix without any sample pretreatment. The Au NRs were synthetized optimizing the synthesis conditions, and then characterized and tested as SERS substrate. The presented results demonstrated that the SERS methodology was able to detect COC in OF with a limit of detection (LOD) as low as 10 ng/mL. This value was five orders of magnitude smaller than the one obtained with Raman spectroscopy (RS) and in the order of the cut-off value (8 ng/mL) established for confirmatory test of COC in OF. Besides, a multivariate

analysis (OPLS-DA) applied on the samples analysed by SERS evidenced that it was possible to discriminate among various COC concentrations. These are quite positive results because even the 1 ng/mL COC concentration sample could be identified as different from the OF sample. In addition, the absence of sample pretreatment and the ease of the proposed method, allowed performing rapid and non-destructive analyses, making the method suitable for *in situ* forensic analyses.

KEYWORDS

Cocaine, Nanoparticles, Gold Nanorods, Oral fluid, Surface Enhanced Raman Spectroscopy, Orthogonal Partial Least Squares to Latent Structures-Discriminate Analysis (OPLS-DA).

ABBREVIATIONS

COC	Cocaine
NP	Nanoparticle
NR	Nanorod
NS	Nanosphere
OF	Oral Fluid
SERS	Surface Enhanced Raman Spectroscopy
SPR	Surface Plasmon Resonance
TEM	Transmission Electron Microscopy
UV	Ultraviolet
OPLS-DA	Orthogonal Partial Least Squares to Latent Structures-Discriminate Analysis

1. Introduction

Surface-enhanced Raman spectroscopy (SERS) is a highly sensitive and selective variant of the Raman spectroscopy (RS). In SERS, the sample is deposited on a metallic surface, usually gold and/or silver nanoparticles (NPs), and the useful Raman signal produced is enhanced by the electromagnetic interaction of the light with the metals. This interaction produces large amplifications of the laser field through excitations generally known as "plasmon resonances" [1]. The resonance condition is determined from the absorption spectroscopy and depends on the shape, size, and dielectric constants of both the metallic NPs and the surrounding material. As the shape or size of the NPs changes, the surface geometry changes causing a shift in the electric field density on the surface [2].

Many shapes of noble metal NPs have been synthesized [3-8], but in the last decades, gold nanorods (Au NRs) have attracted great attention. This is due to the ease of preparation, the large number of synthesis methods available, and the rational control over the aspect ratio (length/width), which is primarily responsible for the change in their optical properties [8-11].

The anisotropic growth of the Au NRs results from facet-selective gold deposition promoted by the silver ions, which adsorb to gold seeds by an underpotential deposition mechanism. However, during the growth, it is possible that the gold deposition on the seeds surface does not occur heterogeneously, and so nanospheres (NSs) are formed instead of NRs. The NRs aspect ratio can be increased to a certain extent, up to 4.5, by increasing the silver concentration, while the absence of silver in the synthesis process results in a poor yield of Au NRs. Thus, the plasmon resonance can be tuned across the visible region by changing the aspect ratio. Moreover, the increase in the intensity of the

surface plasmon resonance absorption leads to an enhancement of the electric field [2, 12].

To profit from the enhancement effect, the sample must be adsorbed on the metal surface, or at least be very close to it, that is, at a maximum distance of typically ~10 nm. The SERS signal can then achieve a scattering above eight orders of magnitude greater than the RS signal [1]. Consequently, SERS can be employed as a sensitive technique to detect very low concentrations of a wide range of compounds in different matrices.

From a forensic point of view, the detection of illicit drugs in biological fluids is actually an issue of primary importance. In particular, in this work, the attention was focused specifically on the detection of cocaine (COC) in oral fluid (OF). COC, which is the second most consumed drug all over the world, after marijuana, easily degrades in aqueous environments, thus it can be found in almost all biological fluids. OF provides a convenient and accurate alternative to urine and blood as a matrix for testing therapeutic and illicit drugs consumption. OF is relatively clean because is colourless, and it can be collected in a simple and non-invasive manner. However, differently from other bodily fluids, only a small amount of sample is collectable. Until now, the majority of the approaches for detecting drugs of abuse in OF are based on immunological procedures or chromatographic techniques coupled with mass spectrometry [13]. The main drawback of using immunological tests, employed for presumptive screening, is the considerable probability to obtain false positives or false negatives. On the other hand, using chromatography coupled to mass spectrometry, confirmatory analysis can be made, since this hyphenated technique is highly sensitive and selective, but it is time-consuming due to the method requirements and the need of sample pretreatment. For these reasons, recently, various spectroscopic approaches are being developed to perform confirmatory

tests in a relatively short time, although they are still poorly applied for illicit drugs detection in OF [13].

As far as the authors know, up to date, only few works [14-17] have been reported about the specific detection of COC in OF by SERS. In all cases, gold- and silver-doped sol-gel were utilized as substrates, needing a complex system of capillaries and a sample pretreatment. Those methods had poor reproducibility and bad reusability of the SERS supports after few cycles. Recently, illicit drugs (COC, THC, heroin, and oxycodone) were identified in both aqueous and OF samples. This was done with a reusable microchip SERS sensor, produced by an electric field-guided assembly process of colloidal silver nanoparticles into nanodendrites onto a silicon surface [18]. Moreover, an accurate quantification of COC was obtained by applying spectral processing and multivariate analysis, in particular the Principal Component Analysis (PCA) coupled with Support Vector Machine (SVM) modelling, for the discrimination between different sample classes. However, the Raman detection of COC in the limit of 100 ng/mL needed a previous crash out of the OF proteins.

This work, focused on exploring the capability of SERS to qualitatively detect COC in non-pretreated OF samples, by employing a new solid substrate made of Au NRs, specially designed for this purpose. The final aim was to demonstrate that it is possible to detect ultratraces of COC in OF and achieve very low LODs while using a relatively simple analytical approach, without pretreating the samples. This possibility will allow performing rapid, confirmatory, and non-destructive analyses, making the developed approach very useful for practical applications in the in forensic field.

2. Materials and methods

2.1. Reagents and samples

The cetyltrimethylammonium bromide (CTAB), tetrachloroauric (III) acid ($HAuCl_4$), sodium borohydride ($NaBH_4$), silver nitrate ($AgNO_3$), and ascorbic acid, used for the synthesis of the Au NRs were purchased from Sigma-Aldrich (St. Louis, MO, USA). The COC.HCl was obtained from Lipomed (Arlesheim, Swiss, EU), and the OF samples were donated by a non-consumer volunteer.

The reference aqueous solutions of COC and COC-doped OF samples were prepared by dissolving solid COC.HCl in water and OF, respectively. Their drug concentrations ranged from 1 mg/mL to 1 ng/mL.

2.2. Nanorods synthesis

Au NRs were synthetized employing a seed-mediated, surfactant assisted method firstly reported elsewhere [19] with slight variations. The process is based on the initial preparation of Au seeds in an aqueous solution of CTAB 0.1 M, $HAuCl_4$ 0.25 mM, and $NaBH_4$ 0.6 mM, which was maintained under gently stirring during 2 min. Different volumes of the previously synthesized Au seeds were then added to a growth solution. This mixture consisted of CTAB 0.1 M, $HAuCl_4$ 0.5 mM, ascorbic acid 0.55 mM, and $AgNO_3$, at the different concentrations tested, in a proportion of 1 μL of Au seeds per mL of growth solution. The $AgNO_3$ and Au seeds concentrations were optimized in order to obtain NRs with an aspect ratio that allowed tuning the plasmon resonance to the excitation wavelength of the laser employed for the RS and SERS analyses. In the study, three concentrations of $AgNO_3$ (0.04, 0.075, and 0.15 mM), and five different volumes of Au seeds (1, 2, 5, 10, and 20 μL), added per mL of growth solution, were compared. The CTAB served to coat the seeds surface as a bilayer, preventing the aggregation and aiding the NRs growth by facet-sensitive surface adsorption. The ascorbic acid was used

as a weak reducing agent that induced heterogeneous gold deposition at the surface of the seeds [12]. In all cases, the Au NRs were left to grow during 4 h under stirring at 28 °C. Finally, in order to separate NRs from the homogeneously grown NSs, the obtained NPs solution was doubly centrifuged [20], first at 10630 rpm for 30 min, and subsequently at 6000 rpm for 30 min.

2.3. Instrumental

The ultraviolet-visible (UV-VIS) spectra were collected with a Kontron Uvikon 941 Plus spectrophotometer (St. Quentin en Yvelines, France, EU) operating in the 400 - 900 nm range. For the UV-VIS analyses, 3 mL of the Au NRs solution were transferred and directly analysed into a standard Quartz cuvette with a 10 mm light path.

The transmission electron microscopy (TEM) images were taken with an EM-10C microscope (Carl-Zeiss, Thornwood, NY, USA) with a field emission gun operating at 80 kV. For the TEM analyses, a drop of the Au NRs solution was placed on a formvar coated copper grid, then, it was let dry, and finally analysed. The obtained micrographs were treated with the ImageJ software (ImageJ Net, worldwide open source) and the histogram representing the size distribution was made with the OriginPro 8.6 software (Originlab, Northampton, MA, USA).

The RS and SERS spectra were collected with a DXRTM Raman Microscope (Thermo Scientific, Waltham, MA, USA) using a 780 nm excitation wavelength laser, and the 50x magnification lens. The spectral region of interest was set from 600 to 1500 cm^{-1}. All the samples were measured with the following settings: 10 scans with a 10 s duration, 10 mW laser power, and a 50 μm slit aperture. The RS characterization of the Au NRs was carried out as follows: a 5 μL drop of the Au NRs solution was deposited on an aluminium surface, and was let dry before the analyses. The Au NRs solutions were always freshly

prepared, and had an average concentration of 95.3 mg/mL. Nonetheless, after being stored for 15 months at 4 ºC, the solutions were still stable, with the same optical absorption spectra.

Finally, to study the efficiency of the synthetized Au NRs, for the SERS analyses, a 5 μL drop of each freshly prepared solution of COC in water or in OF was deposited onto an individual dry Au NRs stain. For the comparative analyses with RS, the 5 μL drop of each freshly prepared solution of COC was placed directly on the aluminium surface. Either case, the COC solutions were allowed to dry before the analyses.

In all cases, the measurements were randomly collected, considering a large number of spectra in a wide area of the ring spot, which was originated by the differential evaporation rates across the liquid sample drops. Chemical maps obtained by Raman experiments showed that COC was present mostly in the drop border. Figure S1 illustrates the ring formed after drying the OF drop, in a so-called "coffee ring" pattern.

2.4. Data acquisition and treatment

All the spectra were collected with the Omnic for dispersive Raman 8.3.103 software (Thermo Scientific, Waltham, MA, USA). The fluorescence effect was diminished by means of a 3rd-order polynomial baseline correction, whilst the noise interference was reduced using an 11-point smoothing algorithm. Both functions were built-in the Omnic software.

The method's LOD for detecting COC was estimated by monitoring the gradual disappearance of the characteristic COC bands in the different gathered spectra. This was done until the selected bands (1000 cm^{-1} (SERS) or 1005 cm^{-1} (RS) for the water matrix; and 1024 cm^{-1} (SERS) or 1030 cm^{-1} (RS) in the OF matrix) reached a signal/noise ratio

of approximately (S/N ≥ 3), for both RS and SERS analysis. As a simplification, we indicated LOD as the analyte concentration which is large enough to produce a signal (band) at least three times larger than the noise recorded in the absence of the analyte (blank signal). Both, the analyte and noise signals were evaluated manually considering the height of the selected bands and their baselines, respectively.

Furthermore, multivariate analysis was performed on the collected SERS spectra of the COC in the OF samples. As a common practice, various chemometrics tools are commonly used for modelling and help explaining the behaviour of several kind of chemical and biological data. Some of those methods are principal components analyses (PCA), linear discriminant analysis (LDA), partial least squares to latent structures (PLS), orthogonal PLS (OPLS), and others. Based on PLS, the OPLS and OPLS discriminate analysis (OPLS-DA), rotates the model allowing observing the correlated variation, which is related to the class separation (discrimination), in the first predictive component. The uncorrelated variation, which is not related to the class separation, emerges in the orthogonal components [21]. Although the prediction information offered by OPLS is essentially the one given by PLS, the idea of predictive and orthogonal components help during the interpretation of the OPLS-DA model. The OPLS-DA method was used for trying to discriminate between the different OF solutions doped with various cocaine concentrations, in the SERS measurements. This multivariate analysis was performed using SIMCA (Sartorius Stedim Biotech, Aubagne, France). The spectral data was previously centred and scaled (Pareto), and the software was set to calculate the boundaries with 95 % probability [22] to compensate for any magnitude unbalance and/or variance that could exist. This enabled to eliminate any weight due to the variables or observations magnitude. The analysis was carried out using a non-linear iterative partial least squares (NIPALS) algorithm, cross validation with uncertainty test, and 1/SDev as

weighing. Because OPLS-DA is sensitive to the model complexity [22], cross-validation (CV) was set to estimate the relevant number of components in the OPLS models.

3. Results and discussion

3.1. Plasmon resonance tuning

As mentioned before, different $AgNO_3$ concentrations (0.04, 0.075, and 0.15 mM) and Au seeds volumes (1, 2, 5, 10, and 20 μL, added per mL of growth solution) were tested in order to obtain the best NRs aspect ratio for shifting the plasmon resonance into the excitation wavelength of the employed laser. The UV-VIS spectroscopy was used for the comparison since it is one of the most widely used techniques for the structural characterization of NPs. The optical absorption spectra of metallic NPs are dominated by surface plasmon resonances (SPRs), which shift according to the NPs size. The position and shape of the plasmon absorption are strongly dependent on the particles size, composition, dielectric medium, and surface adsorbed species [23]. For NRs, the analyses usually reveal two plasmons: the transversal SPR band, which does not depend on the aspect ratio and is approximately at the same wavelength of the NSs' SPR; and the longitudinal SPR, which is variable and increases with larger aspect ratios. It was observed that, for all the different $AgNO_3$ concentrations, the added Au NRs volume did not really affect the spectrum profile (figure not shown). The **Figure 1** shows the UV-VIS spectra of the Au NRs obtained at a constant volume of Au seeds (1 μL per mL of growth solution) while varying the $AgNO_3$ concentration.

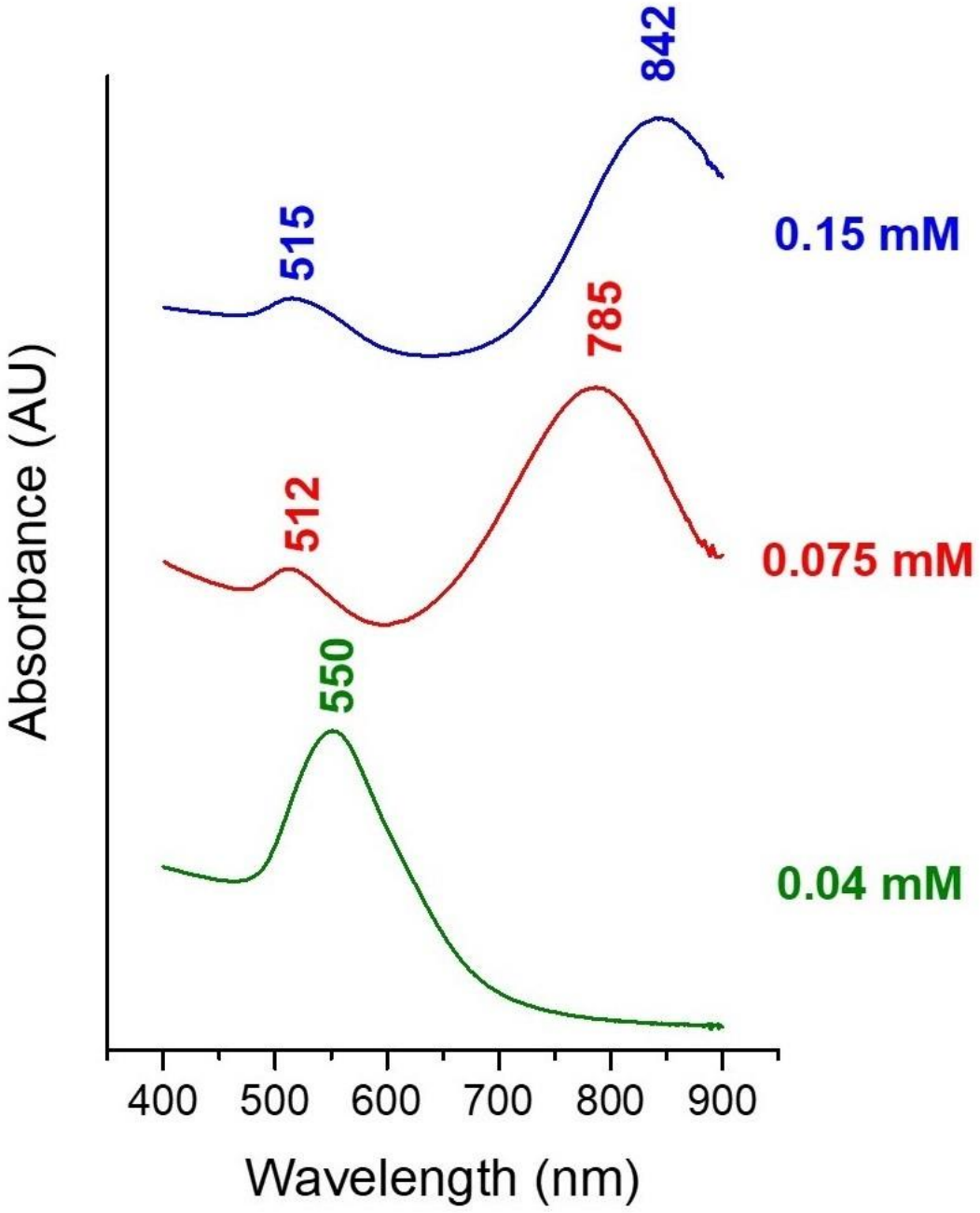

Figure 1. UV-VIS spectra of the Au NRs obtained varying the $AgNO_3$ concentration and keeping constant the volume of Au seeds (1 μL per mL of growth solution).

In all cases, it can be observed that the first plasmon corresponds to the one of the NSs and/or to the transversal one of the NRs. On the contrary, the longitudinal plasmon of the NRs did not even appear at the smallest $AgNO_3$ concentration (0.04 mM), which means

that no NRs were formed. At higher $AgNO_3$ concentrations (0.075 and 0.15 mM), the longitudinal plasmon could be observed instead, and their corresponding wavelength values increased with increasing the salt concentration.

The parameters giving the nearest NRs plasmon were selected considering the excitation wavelength of the laser employed (780 nm). Therefore, in order to synthetize the Au NRs for this study the following conditions were fixed: 0.075 mM $AgNO_3$ concentration, and 1 μL of Au seeds per mL of growth solution.

3.2. Nanorods characterization

Figure 2 shows some characteristics features of the bare Au NRs: TEM image (A), their size distribution (B), and their resultant Raman spectrum (C).

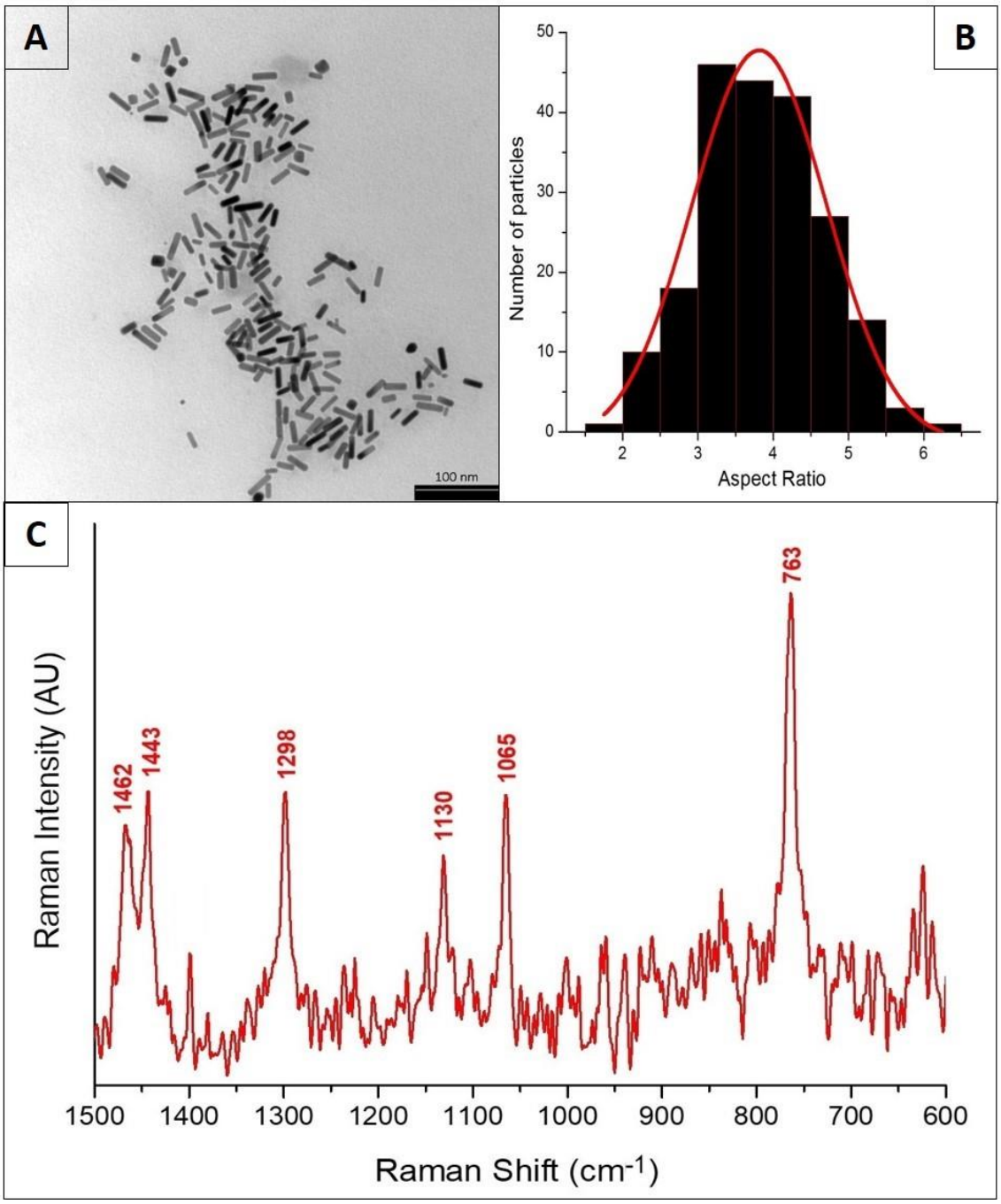

Figure 2. Characterization of Au NRs. TEM image of the NRs (A), their size distribution (B), and corresponding Raman spectrum (C).

TEM gives important information about the morphology, shape, size, and size distribution of the NPs. Here, the TEM image (Figure 2A) shows the presence of the Au NRs, with an average length of about 23 nm, and an average width of about 6 nm. In addition, the photomicrograph also shows the presence of Au NSs with a mean diameter of about 9

nm, formed by the isotropic growth of the initial gold seeds. The size distribution of the NRs was then represented as a function of the aspect ratio, giving a mean value of about four (Figure 2B).

The RS spectrum of the bare Au NRs (Figure 2C) was collected as reference, which allowed recognizing the Au NRs signal and distinguishing it from the COC and OF signals. We included in the supporting material that raw spectrum without any baseline correction (Figure S2). Most of the significant bands that appeared at 1462, 1443, 1298, 1130, 1065, and 763 cm^{-1}, were identified as characteristic of the Au NRs.

3.3. Cocaine ultradetection

In previous works, we studied in detail the Raman spectra of COC in water and in OF [24, 25]. The assignment of the COC and OF Raman bands were based on literature reports. Considering this, none of the characteristic spectral bands obtained for the bare Au NRs interfered with the dominant bands of COC or OF [16, 24, and 25].

Figure 3 shows the comparison between the RS and the SERS spectra of the COC aqueous solutions, at the corresponding lowest COC concentrations detectable in our experiments. The supportive **Figure S3** shows the same spectra without any data treatment.

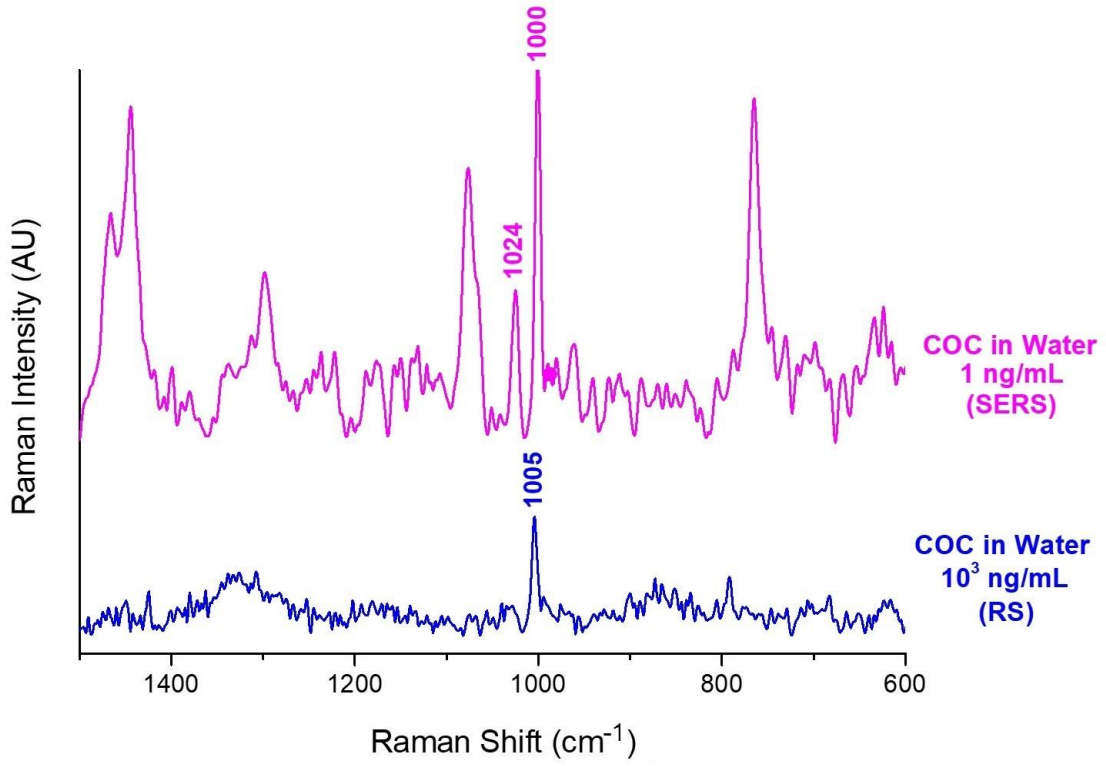

Figure 3. Comparison between the RS and SERS spectra of an aqueous solution of COC. The bands at 1462, 1443, 1300, 1074, and 763 cm^{-1} in the COC in water SERS spectrum correspond to the bare Au NRs.

In both cases, two of the most characteristic bands of COC were used to estimate the LODs as referred above in the experimental section (2.4). These bands appeared at about 1005 and 1030 cm^{-1} in the RS spectra, and at about 1000 and 1024 cm^{-1} in the SERS spectra. Those are attributed to the symmetric and asymmetric phenyl ring breathing modes, respectively [24]. Interestingly, these two bands are also characteristic for benzoylecgonine, which is the main COC degradation product in the liver, and whose transformation in real samples would not have an effect on the detection results. On the other hand, due to surface interactions, SERS spectra are often different from the corresponding RS spectra. These interactions enhance various vibrational modes to different extents, thus shifts or changes in the relative intensity of the bands can be observed [26]. Since water does not show characteristic bands in the RS or SERS spectra

between 600 and 1500 cm^{-1}, it can be considered that COC was present until at least one of the two bands was still observable. The criterion was a signal to noise ratio of at least three. Consequently, it could be noted that with RS, COC was detectable in water at a concentration of 1 μg/mL (10^3 ng/mL), since the band at 1005 cm^{-1} could still be observed (Figure 3). With SERS, instead, the drug was detectable even at a concentration of 1 ng/mL, with both bands, at 1000 and 1024 cm^{-1}, clearly visible (Figure 3). In addition, the SERS spectrum of COC in aqueous solution, showed bands at 1462, 1443, 1300, 1065, and 763 cm^{-1}, which are assigned to the bare Au NRs (compare Figure 2C and Figure3).

Afterwards, the same analyses were directly carried out on the OF samples doped with COC. Differently from water, in the studied range, the OF showed characteristic bands in RS and SERS spectra, which could overlap the COC signal [28, 29]. Thus, in this case, the first step was to collect the undoped OF spectra. **Figure 4** shows the RS and the SERS spectra of an OF sample. The supporting Figure S4 shows the average and standard deviation spectra of the raw data for the OF matrix.

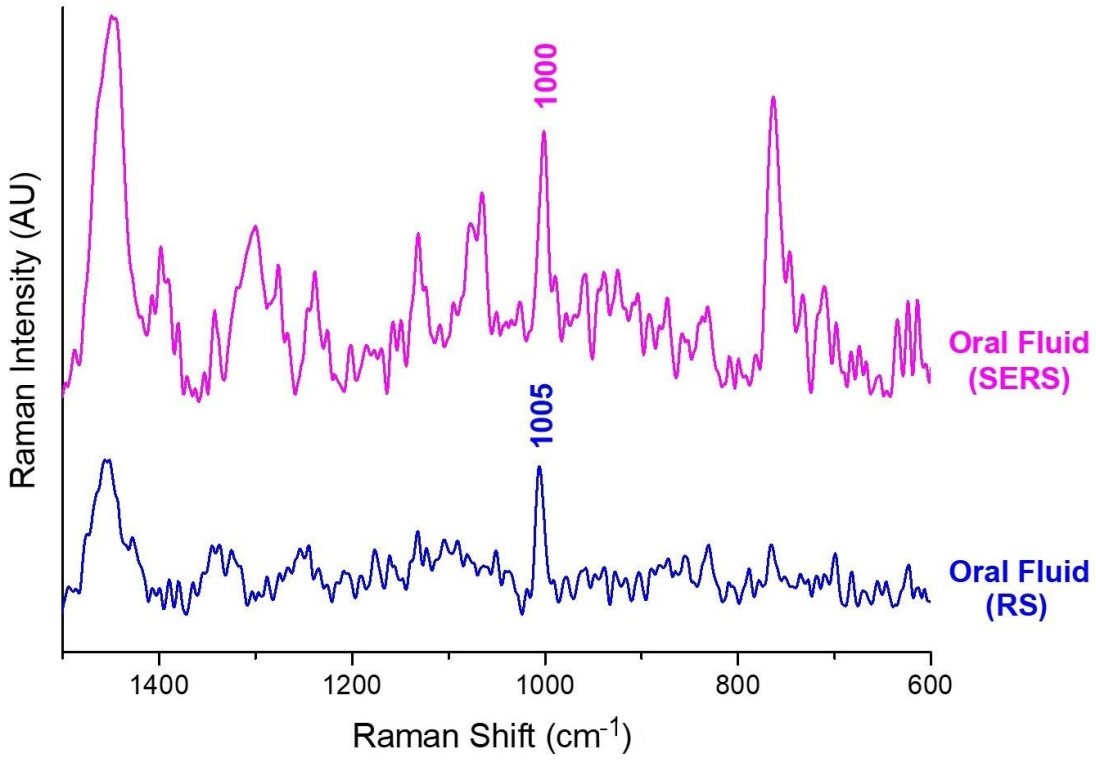

Figure 4. Comparison between the RS and SERS spectra of OF matrix.

It is interesting to note that, in contrast to other bodily fluids such as blood or semen, the Raman spectrum of dry OF varies considerably from donor to donor [28]. In fact, Sikirzhytski *et al* studied the spectral components of OF focusing on the significant contribution from chemical groups like glycoproteins, and mucin components such as acetate, which appeared as bands at about 1295 and 1434 cm^{-1} [28, 29]. On the other hand, the Au NRs bands at 1462 and 1443 cm^{-1} run into the CH stretching band at about 1444 cm^{-1} of the OF spectrum (Figure 4). Thus, as it could be noted in the RS and SERS spectra, OF showed a characteristic band appearing at 1005 and 1000 cm^{-1}, respectively (Fig. 4). This band could be attributed to the vibrational modes of proteins commonly present in that OF matrix, and, in particular, to their aromatic rings breathing modes [28, 29]. Regrettably, as before observed, these bands appear exactly as one of the characteristic COC bands, which corresponds to the symmetric breathing vibrational mode of the

phenyl ring. Thus, in this case, it was not reliable to focus on them to conclude the possible presence of COC band features. Instead, in the RS and SERS spectra, it was necessary to consider the COC bands appearing at 1030 and 1024 cm^{-1}, respectively. For this reason, the variation of the band intensity with the concentration was monitored focusing on the 1040 - 990 cm^{-1} range. Hence, **Figure 5** compares the OF spectrum against the spectra corresponding to the average spectra of COC in OF samples at different compositions. The spectra went through a baseline correction and smoothing of the noise.

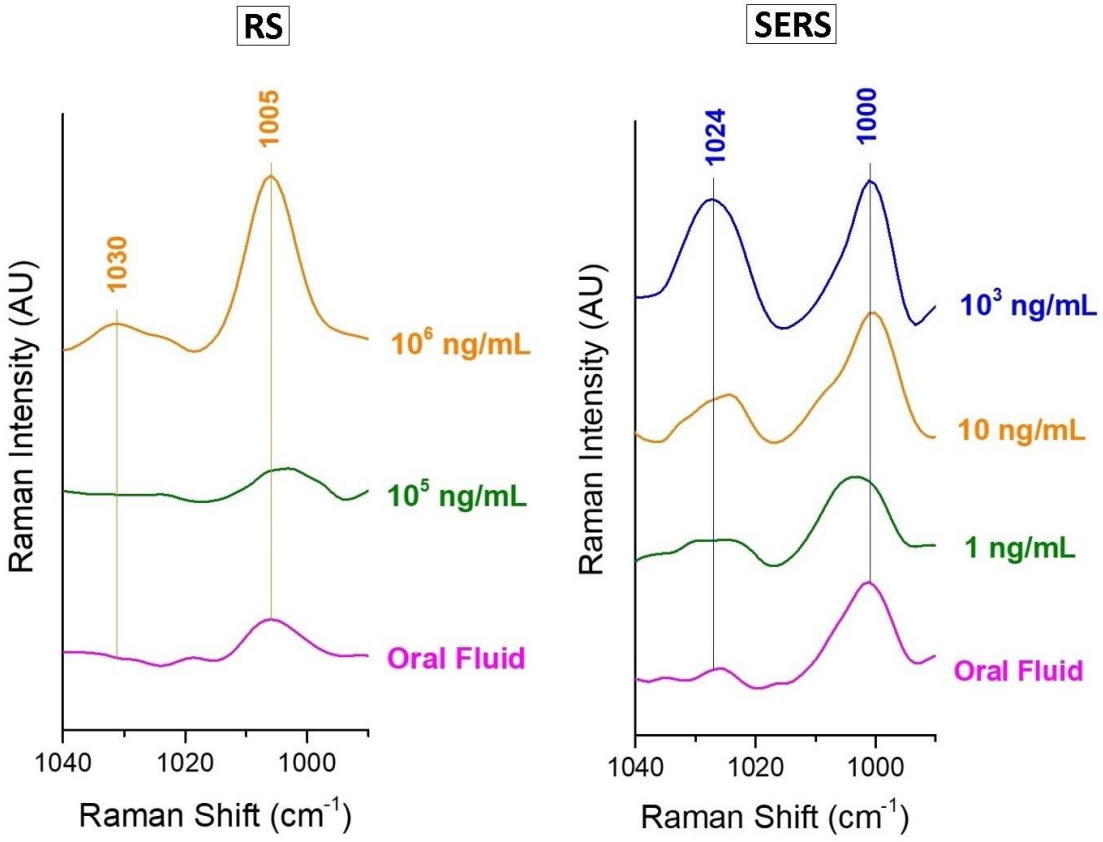

Figure 5. Limits of detection achieved for COC in OF by RS and SERS, compared to the OF spectrum.

The LOD were estimated by monitoring the gradual disappearance of the selected COC band in the different spectra until that band reached a S/N ≈ 3. This method in detecting COC in OF was successful used before in Ultraviolet Resonance Raman spectroscopy studies [25]. As is evident for RS in Figure 5, COC was only observed at the highest concentration, 1 mg/mL (10^6 ng/mL). On the other hand, with SERS, COC was observed in OF at a concentration as low as 10 ng/mL, that is, five orders of magnitude lower than the one detected with RS. However, for this sample, was necessary to collect great number of spectra. In some zones, in fact, the COC signal was completely overtopped by the one of the matrix. This could be explained considering that mucins and other OF components could trap the drug molecules and clog the substrate pores, blocking the metal surface.

Beyond the LODs estimation by observing the decreasing bands intensity, additionally, multivariate analysis was performed on the SERS analysis for the same samples given in Figure 5. Further than gaining a dimensional reduction of the COC samples spectra, OPLS-DA was applied for discriminating the various COC concentrations used in the SERS study. Hence, Figure 6 shows the 3D Scores Scatter plot from the OPLS-DA model used on the OF and the COC samples spectra at various concentrations. This method could be used for quantification by enlarging the number of drug concentrations, samples replication, and the inclusion of OFs from different donors. Interestingly, it can be seen that each sample group (class) formed its own cluster, even with only five spectra (replicates) for every class/cluster. Surprisingly, even the 1ng/mL COC concentration sample could be identified as different from the OF sample. This is worth mentioning since this technique would already help during the COC identification and quantification. In the literature, PCA was used to differentiate illicit drugs and detect COC reaching a LOD of 100 ng/mL of COC in OF, which is two orders of magnitude higher than the value obtained in this work [18].

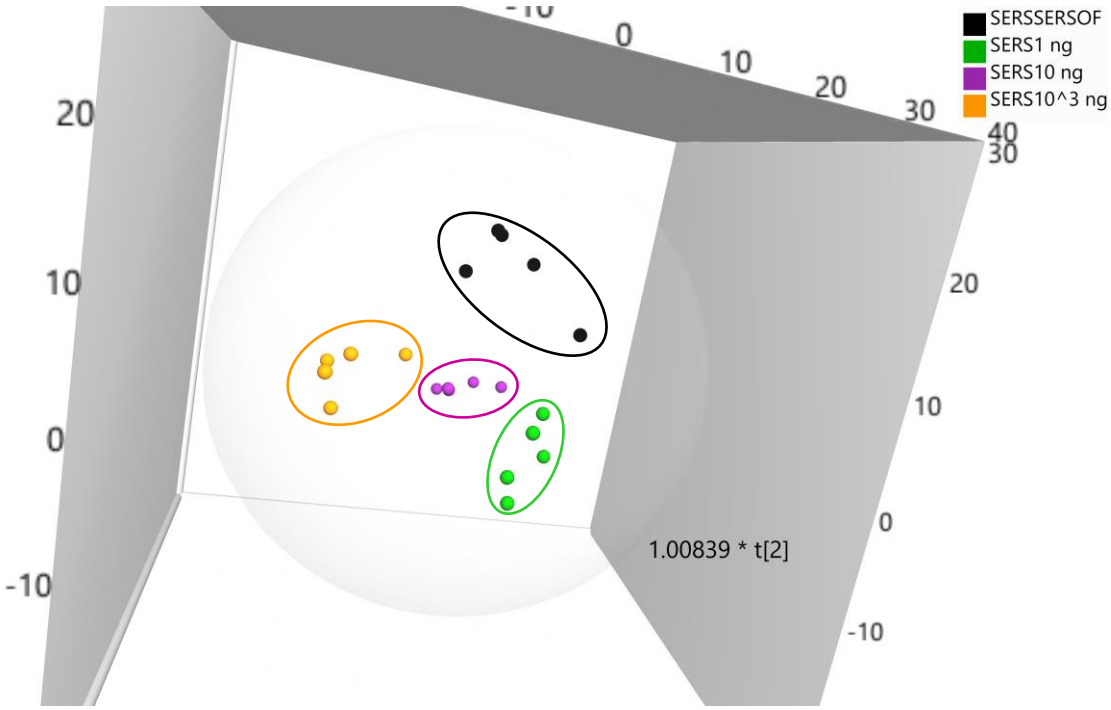

Figure 6. Three-dimensional scores scatter plot from the OPLS-DA model applied to the SERS spectra from the COC in OF samples and OF matrix. Each class (cluster) projected in the t[1]-t[2]-t[3] planes consisted of five spectra. The various COC concentrations were as follows: Black (top) = OF, Green (right) = 1 ng/mL, Violet (middle) = 10 ng/mL, and Orange (left) = 10^3 ng/mL.

It is remarkable that the LOD here observed is the lowest one achieved up to date, for COC in OF with SERS. In fact, as far as the authors know, until now the lowest reported LOD for COC in OF corresponded to 25 ng/mL [17], although a complex analytical system had to be used. In that case, the SERS effect was provided by metallic NPs in form of gold- and silver-doped sol-gel, which were incorporated in a porous glass structure immobilized in a glass capillary. In this case, a, sample pretreatment comprised a chemical and physical separation, and a solid-phase extraction was necessary to recover the analyte drug from the matrix.

4. Conclusions

This work studied the capability of SERS to detect ultratraces of COC in OF. The enhancement, in this case, was provided by a SERS substrate made of *ad-hoc* Au NRs. The aspect ratio of the synthetized Au NRs was expressly optimized to tune their plasmon resonance absorbance to match the excitation wavelength of the laser used for RS and SERS analyses.

Non-pretreated COC-doped OF samples were analysed, and their SERS spectra obtained and compared with the corresponding RS spectra collected with the same instrumental parameters. It was clearly noted for SERS, that the detection of COC was significantly improved. In fact, comparing the LODs achieved with RS and SERS, it was observed that the COC concentration detected in OF by SERS was five orders of magnitude lower than the one detected by RS. Furthermore, as far as the authors know, the LOD obtained here (10 ng/mL), is the lowest achieved until now with spectroscopic techniques. In addition, the multivariate analysis (OPLS-DA) showed that it was possible to discriminate among the several COC concentrations (from 1 ng/ mL to 10^3 ng/ mL) analysed by SERS. These are quite positive results because even the 1ng/mL COC concentration sample could be identified as different from the OF matrix.

In conclusion, this work proved that it is possible to successfully detect COC ultratraces in OF, by using a simple solid Au NRs substrate. The great advantage of the proposed approach is that no sample pretreatment was necessary, because the samples were deposited on the SERS substrate directly as they were prepared. In this study, the inconvenience of the high heterogeneity of the dry OF samples caused by the complex OF composition, was easily dealt with collecting a great number of spectra, randomly along the crown of the dry OF drop. In previous works reported in literature, this problem was solved instead by using complex analytical systems and sample pretreatments, such as extraction or preconcentration.

For a future implementation, simple SERS substrates need to be prepared prior their adaptation to portable devices, similar to the ones already on the market. This approach will require to deposit a small amount of OF directly on the SERS substrate, and it could allow performing easy and rapid analyses, thus obtaining confirmatory results also for *in situ* controls, such as drug controls to drivers or attention to overdose in hospital care. A further study to improve the Au NRs surface homogeneity will be necessary before the implementation. This could be particularly interesting in the forensic field, considering that the low LOD obtained (10 ng/mL) is in the order of the cut-off value established for confirmatory tests of COC in OF.

Acknowledgments

The authors acknowledge for the Projects CCG2015/EXP-028, MAT2017-83111R and B2017/BMD-3867 RENIM-CM. V. D'Elia thanks the University of Alcalá for the grant offered.

References

[1] Le Ru, E.C., and Etchegoin, P.G. (2009) Chapter 4: SERS enhancement factors and related topics. In Principles of Surface-Enhanced Raman Spectroscopy, Le Ru E.C., Etchegoin P.G., Eds., Elsevier, Amsterdam, pp. 185 264. (DOI:10.1016/B978-0-444-52779-0.00007-6)

[2] Eustis, S., El-Sayed, M. (2006) Why gold nanoparticles are more precious than pretty gold: Noble metal surface plasmon resonance and its enhancement of the radiative and nonradiative properties of nanocrystals of different shapes, Chem. Soc. Rev. 35: 209-217. (DOI: 10.1039/B514191E)

[3] Hao, E., Schatz, G., Hupp, J. (2004) Synthesis and optical properties of anisotropic metal nanoparticles, J. Fluoresc. 14: 331-341. (DOI: 10.1023/B:JOFL.0000031815.71450.74)

[4] Burda, C., Chen, X., Narayanan, R., El-Sayed, M. (2005) Chemistry and properties of nanocrystals of different shapes, Chem. Rev. 105: 1025 1102. (DOI: 10.1021/cr030063a)

[5] Xia, Y., Yang, P., Sun, Y., Wu, Y., Mayers, B., Gates, B., Yin, Y., Kim, F., Yan, Y. (2003) One-dimensional nanostructures: Synthesis, characterization, and applications, Adv. Mater. 15: 353-389. (DOI: 10.1002/adma.200390087)

[6] Pileni, M. (2003) The role of soft colloidal templates in controlling the size and shape of inorganic nanocrystals, Nat. Mater. 2: 145-150. (DOI: 10.1038/nmat817)

[7] Jin, R., Cao, Y., Mirkin, C., Kelly, K., Schatz, G., Zheng, J. (2001) Photoinduced conversion of silver nanospheres to nanoprisms, Science 294: 1901-1903. (DOI: 10.1126/science.1066541)

[8] Murphy, C., San, T., Gole, A., Orendorff, C., Gao, J., Gou, L., Hunyadi, S., Li, T. (2005) Anisotropic metal nanoparticles: Synthesis, assembly, and optical applications, J. Phys. Chem. B 109: 13857-13870. (DOI: 10.1021/jp0516846)

[9] Link, S., El-Sayed, M. (1999) Spectral properties and relaxation dynamics of surface plasmon electronic oscillations in gold and silver nanodots and nanorods, J. Phys. Chem. B 103: 8410-8426. (DOI: 10.1021/jp9917648)

[10] Link, S., El-Sayed, M. (2000) Shape and size dependence of radiative, non-radiative and photothermal properties of gold nanocrystals, Int. Rev. Phys. Chem. 19: 409-453. (DOI: 10.1080/01442350050034180)

[11] Link, S., Ei-Sayed, M. (2003) Optical properties and ultrafast dynamics of metallic nanocrystals, Ann. Rev. Phys. Chem. 54: 331-366. (DOI: 10.1146/annurev.physchem.54.011002.103759)

[12] Smith, D. K., Korgel, B. A. (2008) The importance of the CTAB surfactant on the colloidal seed-mediated synthesis of gold nanorods, Langmuir 24: 644-649. (DOI: 10.1021/la703625a)

[13] D'Elia, V., Montalvo, G., García-Ruiz, C. (2015) Spectroscopic trends for the determination of illicit drugs in oral fluid, Appl. Spec. Rev. 50 (9): 775 796. (DOI: 10.1080/05704928.2015.1075206)

[14] Inscore, F., Shende, C., Sengupta, A., Huang, H., Farquharson, S. (2011) Detection of Drugs of Abuse in Saliva by Surface-Enhanced Raman Spectroscopy (SERS), Appl. Spectrosc., 65: 1004-1008. (DOI: 10.1366/11 06310)

[15] Farquharson, S., Shende, C., Sengupta, A., Huang, H., Inscore, F. (2011) Rapid Detection and Identification of Overdose Drugs in Saliva by Surface-Enhanced Raman Scattering Using Fused Gold Colloids, Pharmaceutics, 3 (3): 425-439. (DOI: 10.3390/pharmaceutics3030425)

[16] Shende, C., Inscore, F., Maksymiuk, P., Farquharson, S. (2005) Ten minute analysis of drugs and metabolites in saliva by surface-enhanced Raman spectroscopy, Proc. SPIE 6007, Smart Medical and Biomedical Sensor Technology III, 60070S (2005). (DOI: 10.1117/12.633281)

[17] Dana, K., Shende, C., Huang, H., Farquharson, S. J. (2015) Rapid Analysis of Cocaine in Saliva by Surface-Enhanced Raman Spectroscopy, Anal. Bioanal. Tech. 6 (6): 289-293. (DOI: 10.4172/2155-9872.1000289)

[18] Dies, H., Raveendran, J., Escobedo, C., Docoslis, A. (2018) Rapid identification and quantification of illicit drugs on nanodendritic surface-enhanced Raman scattering substrates. Sens Actuators B Chem. 257: 382-388. (DOI:10.1016/j.snb.2017.10.181).

[19] Nikoobakht, B., El-Sayed, M. A. (2003) Preparation and Growth Mechanism of Gold Nanorods (NRs) Using Seed-Mediated Growth Method, Chem. Mater. 15: 1957-1962. (DOI: 10.1021/cm020732l)

[20] Scaletti, F., Kim, C. S., Messori, L., Rotello, V. M. (2014) Rapid purification of gold nanorods for biomedical applications, MethodsX 1: 118 123. (DOI: 10.1016/j.mex.2014.07.007)

[21] Kvalheim, O. M.; Karstang, T. V. (1989) Chemom. Intell. Lab. Syst.7: 39-51. (DOI: 10.1002/cem.1217)

[22] Bylesjö, M.; Rantalainen, M.; Cloarec, O.; Nicholson, J. K.; Holmes, E.; Trygg, J. (2006) J. Chemom. 20: 341-351. (DOI:10.1002/cem.1006)

[23] Pal, S., Tak, Y. K., Song, J. M. (2007) Does the Antibacterial Activity of Silver Nanoparticles Depend on the Shape of the Nanoparticle? A Study of the Gram-Negative Bacterium Escherichia coli, Appl. Environ. Microb. 73 (6): 1712–1720. (DOI: 10.1128/AEM.02218-06)

[24] D'Elia, V., Montalvo, G., García-Ruiz, C. (2016) Analysis of street cocaine samples in nasal fluid by Raman spectroscopy, Talanta 154: 367 373. (DOI: 10.1016/j.talanta.2016.03.077)

[25] D'Elia, V., Montalvo, G., García-Ruiz, C., Ermolenkov, V.V., Ahmed, Y., Lednev, I.K. (2018) Ultraviolet resonance Raman spectroscopy for the detection of cocaine in oral fluid, Spectrochim Acta A. 188: 338-340. (DOI: 10.1016/j.saa.2017.07.010)

[26] Farquharson S., Gift A., Shende C., Inscore F., Ordway B., Farquharson C., Murren J. (2008) Surface-enhanced Raman Spectral Measurements of 5-Fluorouracil in Saliva, Molecules 13(10): 2608-2627. (DOI: 10.3390/molecules13102608.)

[27] Substance Abuse and Mental Health Services Administration (2015) Federal Register, 80(94): 28063. Available at: https://www.gpo.gov/fdsys/pkg/FR-2015-05-15/pdf/2015-11523.pdf (Accessed April 2017).

[28] Sikirzhytski, V., Virkler K., Lednev I. K., (2010) Discriminant Analysis of Raman Spectra for Body Fluid Identification for Forensic Purposes, Sensors 10: 2869-2884. (DOI: 10.3390/s100402869)

[29] Virkler K., Lednev I. K. (2010) Forensic body fluid identification: The Raman spectroscopic signature of saliva, Analyst 135: 512-517. (DOI: 10.1039/b919393f)